A national laboratory of the U.S. Department of Energy
Office of Energy Efficiency & Renewable Energy

National Renewable Energy Laboratory

Innovation for Our Energy Future

The Impact of Coherent Turbulence on Wind Turbine Aeroelastic Response and Its Simulation

Preprint

N.D. Kelley, B.J. Jonkman, and G.N. Scott
National Wind Technology Center

J.T. Bialasiewicz, L.S. Redmond
University of Colorado at Denver

Prepared for WindPower 2005
Denver, Colorado
May 15–18, 2005

Conference Paper
NREL/CP-500-38074
August 2005

NREL is operated by Midwest Research Institute ● Battelle   Contract No. DE-AC36-99-GO10337

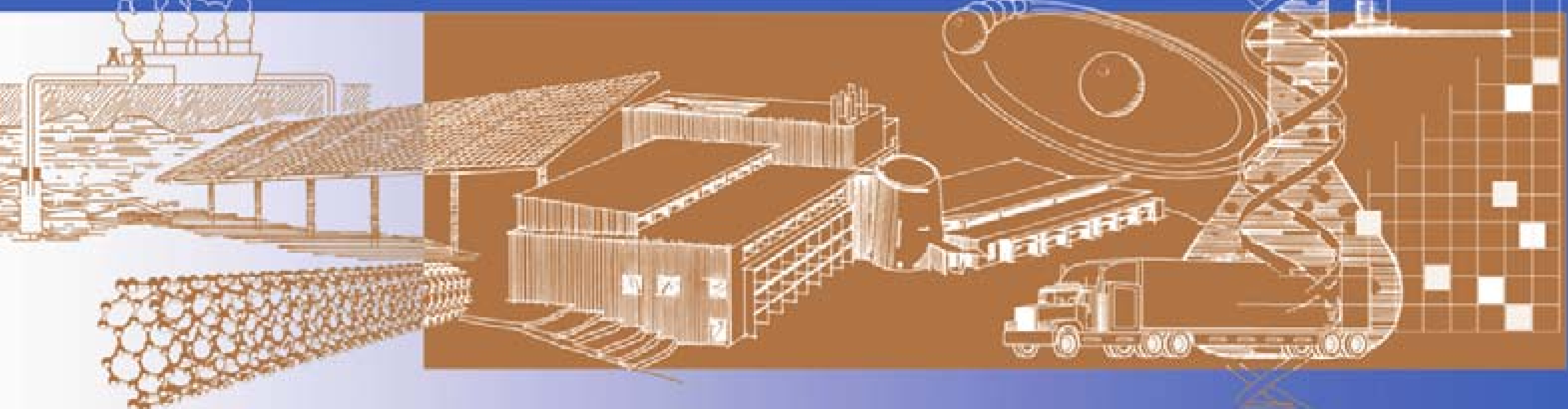

Available electronically at http://www.osti.gov/bridge

Available for a processing fee to U.S. Department of Energy
and its contractors, in paper, from:
U.S. Department of Energy
Office of Scientific and Technical Information
P.O. Box 62
Oak Ridge, TN 37831-0062
phone: 865.576.8401
fax: 865.576.5728
email: mailto:reports@adonis.osti.gov

Available for sale to the public, in paper, from:
U.S. Department of Commerce
National Technical Information Service
5285 Port Royal Road
Springfield, VA 22161
phone: 800.553.6847
fax: 703.605.6900
email: orders@ntis.fedworld.gov
online ordering: http://www.ntis.gov/ordering.htm

Printed on paper containing at least 50% wastepaper, including 20% postconsumer waste

THE IMPACT OF COHERENT TURBULENCE ON WIND TURBINE AEROELASTIC RESPONSE AND ITS SIMULATION

Neil D. Kelley, Bonnie J. Jonkman, George N. Scott
National Wind Technology Center
National Renewable Energy Laboratory
Golden, CO 80401

Jan T. Bialasiewicz, Lisa S. Redmond
Department of Electrical Engineering
University of Colorado at Denver
Denver, CO 80217

ABSTRACT

In this paper, we present a brief overview of our recent research results regarding the impact of organized or coherent inflow turbulence on the dynamic response of operating wind turbines. Previous field experimentation has demonstrated that the greatest structural fatigue damage tends to occur during the nighttime hours from coherent turbulence that develops in the stable, nocturnal atmospheric boundary layer. We have found that under such conditions, intense vertical wind shear and temperature gradients create resonant flow fields that are capable of imparting short-period loading and vibrational energy as wind turbine rotor blades pass through regions of organized or coherent turbulence. This energy is subsequently propagated throughout the remainder of the structure, where it is often locally dissipated. We also briefly discuss our recent progress in developing a numerical simulation that includes such coherent inflow conditions that can be used to excite wind turbine design codes.

INTRODUCTION

One of the goals of the U.S. Department of Energy (DOE) Wind Program is to lower the cost of wind energy produced by land-based utility-scale turbines located in lower wind speed resource areas to $0.03 per kilowatt-hour (kWh). To accomplish its goals, the Wind Program instituted the Low-Wind Speed Turbine Project to help industry develop wind energy technologies capable of capturing the wind resource in these more numerous but less energetic wind regimes that are often nearer to large load centers. Wind energy technologies that can take advantage of the increased wind speeds present at higher altitudes will require larger diameters rotors that rise deeper into the atmospheric boundary layer. The overall trend in recent turbine designs is consistent with this approach as rotors become larger and commensurately sized towers are being built and deployed. This growth has also been accompanied by an increase in structural flexibility that is often further exacerbated by the need to reduce weight. The result has been that the newer, larger turbine designs are also more dynamically active.

Previously in [1] we discussed the potential role of nocturnal low-level jet streams (LLJs) that are prevalent in the areas targeted for potential LWST installations such as the Great Plains. In [2] we discussed that, while nocturnal LLJS provide the benefit of an increased wind resource with height, they also supply the intense vertical wind shears and temperature gradients below the height of the LLJs maximum velocities that feed the development of atmospheric instabilities such as Kelvin-Helmholtz Instability (KHI). As discussed in both [1] and [2], KHI is responsible for creating intense bursts of coherent turbulence in the nighttime (statically stable) boundary layer. During the day, the boundary layer is usually statically *unstable* or *convective* and will not support KHI. Convective motions typically have spatial dimensions much larger than the largest wind turbine whereas coherent motions associated with KHI in a stable boundary layer can be the same size as the turbine rotors or much smaller. KHI occurs when the vertical gradients of temperature and wind speed allow atmospheric wave motions called *billows* or KH waves to develop. The KH billows actually represent a form of *atmospheric resonance* in the turbulent wind field that is controlled by stability (vertical motions being *damped* by negative buoyancy).

KH billows, like water waves, gradually roll up and break. We demonstrated in [2] that the breakdown of a KH billow or wave produces a coherent or organized turbulence structure that is continually evolving. The coherent turbulent region is reasonably well defined in both time and space (*spatiotemporal*) as opposed to a much more random variation seen in what is known as *quasi-homogeneous* or even *homogenous turbulence* (the statistics of the turbulence are independent of spatial position). These coherent structures can be viewed as being superimposed on a much more random turbulent background flow.

IMPACT ON TURBINE BLADES ENCOUNTERING COHERENT STRUCTURES

The evolutionary nature of a breaking KH billow produces a series of bursts of nonstationary turbulence that last only a few seconds. Because the billow has a specific spatiotemporal structure, its turbulent energy resides in more or less discrete frequency bands whose kinetic energy content varies as the breakdown proceeds. A turbine rotor blade passing through such a structure will encounter fluctuating levels of turbulent energy varying in both in time and space (frequency). To observe the dynamic response of such a blade expressed in terms of the time variation of its root flapwise bending load and associated dynamic stress levels, we apply wavelet analysis techniques [3]. This approach allows us to examine not only the time history of the interaction as the blade passes through the coherent turbulent region but the intensity of the induced dynamic stresses occurring at the respective blade modal or natural vibrational frequencies.

Coherent Turbulence Interaction with the WindPACT Virtual Turbine

To apply wavelet analysis techniques to examine the time-varying turbulence/loading response shown in Figure 1, we use numerically predicted root flapwise bending loads derived from a model of a virtual variable-speed 1.5-MW, 3-bladed upwind turbine that has an 85-m hub height and a 70.5-m rotor diameter. This model was originally developed by Malcolm and Hansen [4] as part of the DOE Wind Partnership for Advanced Component Technologies (WindPACT) component study. The calculations were made using an MSC.ADAMS® (Automatic Dynamic Analysis of Dynamic Systems Code [5]) model implementation of a FAST (Fatigue, Aerodynamics, Structures, and Turbulence Code [6]) model of the WindPACT turbine developed by J. Jonkman of the National Renewable Energy Laboratory (NREL). It was necessary to port the FAST version to ADAMS to excite higher modal frequencies that could not be adequately resolved with the limited number of degrees of freedom available in the FAST mechanization. We excited the ADAMS model solution with a portion of the Large Eddy Simulation (LES) of the life cycle of a stationary KH billow developed by the National Center for Atmospheric Research (NCAR) that is discussed more fully in [1] and [2]. To excite the turbine model, we only used the portion of the LES solution in which the KH billow was breaking down and creating the most intense coherent turbulent structures and which eventually died away.

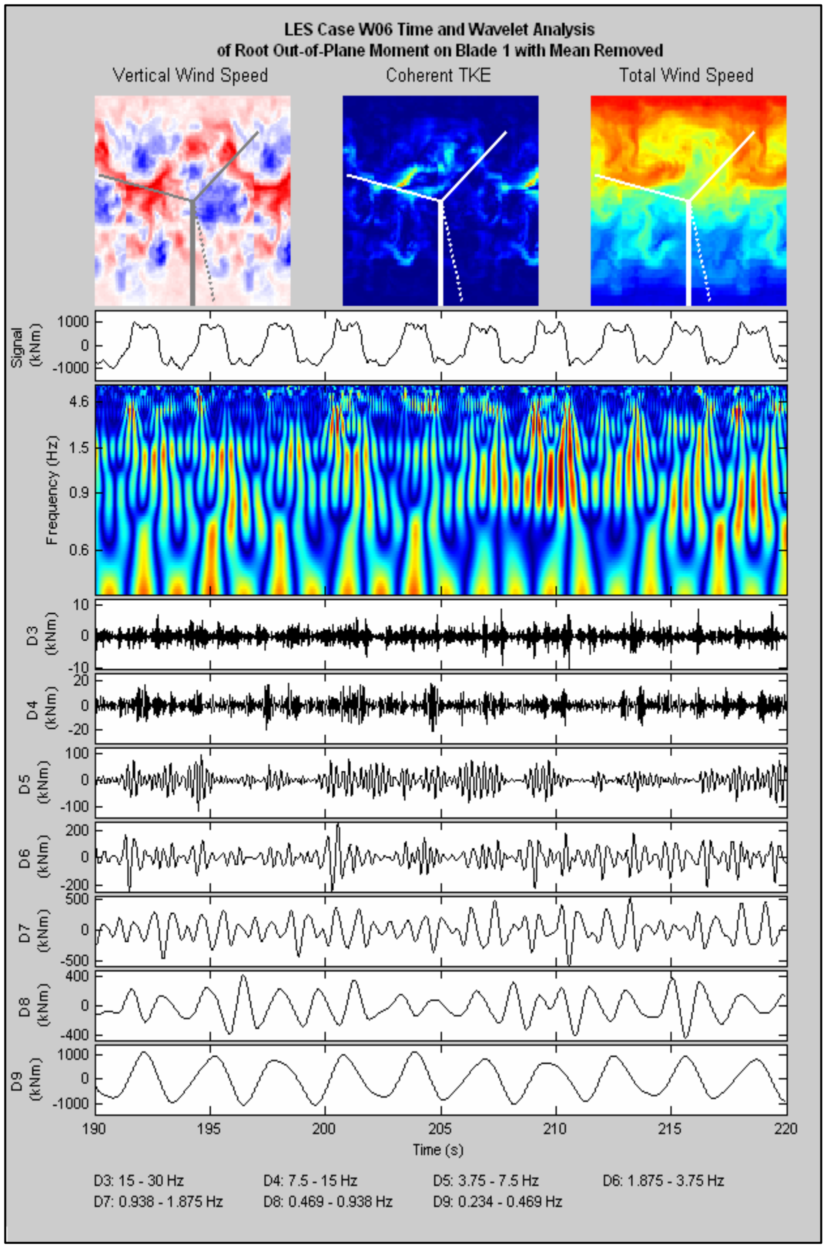

Figure 1. Time-frequency spectral decomposition of the root flapwise load encountering a coherent turbulent structure.

Figure 1 shows the portion of the actively evolving KH billow between 190 and 220 seconds. The left upper window displays the vertical velocity field in the plane occupied by the turbine rotor disk (red is upward and blue is downward motion). The deeper colors represent higher values. The center window depicts the *coherent turbulent kinetic energy* (CTKE or E_{coh})† field with darkest red signifying the regions with the greatest intensity. The upper right window plots total wind speed in the rotor plane with the deepest red depicting high speeds and blue low speeds. The significant vertical wind shear is still evident at this stage (intense blue at the bottom and intense red at the top). At this point in the evolution, note the presence of a considerable number of small-scale structures some of which contain significant CTKE. Note also the relative size of these structures as compared with the rotor dimensions.

† *Coherent turbulent kinetic energy (CTKE or E_{coh}) is defined as $0.5([u'w']^2+[u'v']^2+[v'w']^2)^{1/2}$ where u', v', and w' are the streamwise, crosswind, and vertical eddy (zero-mean) velocity components referenced to a coordinate system aligned with the local flow*

The time series of the blade root flapwise load with the mean removed is plotted immediately below the three upper panels. Note the departure in its shape relative to what may be expected to be much more sinusoidal as a result of the vertical wind shear. The panel immediately below displays the variation of the root load dynamic stress as a function of time and log frequency with the highest frequencies shown at the top. As before, the deepest red color signifies the occurrence of the highest level of dynamic stress energy and dark blue the least. The positions of the darkest red color regions indicate the elapsed time in the record at which they occur and their corresponding frequency content or spectrum. The light blue, yellow, and red regions are associated with the turbine modal or natural vibration frequencies that are being excited at that point in time, and again the deepest red color indicates the greatest level of dynamic stress. The series of plots in the lower portion of Figure 1 represent the time variation of the root flapwise load within seven frequency (detail) bands numbered D3 through D9 A general description of the source of the modal or vibrational frequencies contained in each of the detail bands, including the total number of modes, is listed in Table 1.

TABLE 1. WindPACT Virtual Turbine Calculated Static System Frequencies [7]

Wavelet Detail Band	**Frequency Range (Hz)**	**Vibrational Modes General Characteristics**	**Total Number of Included Modes**	**Number of Blade/Tower Interacting Modes**
D9	0.234 – 0.469	1-P, Tower bending	2	0
D8	0.469-0.938	2-P	0	0
D7	0.938-1.875	Blade 1st bending	3	0
D6	1.875 – 3.75	Blade 2nd bending	5	2
D5	3.75 – 7.5	Blade, blade/tower	3	1
D4	7.5 – 15	Blade, blade/tower	7	5
D3	15 – 30	Blade, blade/tower	7	3

The detail bands D3-D9 in the lower portion of Figure 1 depict the time variation of the amplitude of the root flapwise load that occurs within the frequency range associated with each. For example, the variation shown within the lowest frequency Band D9 is sinusoidal-like and reflects the contribution to the load occurring between 0.234 and 0.469 Hz. From Table 1 we see that the variation in the load with each blade revolution (~0.342 Hz or 1-P) and two tower bending modes are the likely contributors to the observed waveshape.

Clearly the character of the waveforms changes as the frequency ranges or, equivalently, the center frequencies of the detail bands rise. In Bands D6, D5, D4, and D3, the waveforms increasingly take on the characteristic of *transient damped oscillations* whose lengths become shorter as both the frequency bandwidth and center frequency of the bands increase. This indicates that the loads within these frequency bands are being applied more as an impulse as opposed to a load variation that is occurring over one blade revolution (1-P); i.e. in Band D9 and at the 2-P rate in Band D8. While the peak amplitudes of the load time histories in Bands D6 through D7 decreases, the number of stress reversals increase as the rotor passes through coherent turbulent structures. Because of the nature of the load application and the existence of the small values of structural damping seen in most large turbines, it is likely that there is a significant transient storage of vibrational energy that must be dissipated. It also seems likely that, under these circumstances, the possibility of modal dynamic amplification may exist, which could possibly contribute to lower than designed component service lifetimes.

Flux of Coherent Turbulent Kinetic Energy Into Turbine Structure

The source of the short-period, transient loads depicted in the higher frequency detail bands in Figure 1 are the coherent turbulent structures through which the rotor blades pass. In [3], we used wavelet analysis tools to demonstrate that a blade encountering a coherent turbulent structure induces transient loads that couple energy into the rotor natural vibration (modal) frequencies. We demonstrate the process in which we examine the *non-stationary* time and frequency transport or flux of coherent turbulent energy (CTKE) from the velocity field to the rotor blade manifested as variations in the blade dynamic pressure or q_c at a given spanwise location. We use the wavelet technique of the *co-scalogram,* as applied by Gurley and Kareem [8], to map the time-frequency variation of the energy flux from the excitation (CTKE) to the response (q_c) variable. It is analogous, in many respects, to Fourier cross-spectral analysis but with the variation in spectral energy resolved not only in frequency but also as it occurs (in time).

We excited the WindPACT turbine model with the breaking portion of the LES KH billow and obtained the individual time series of the blade dynamic pressure at the 78% span element and the velocity field CTKE in the inflow at that location. The co-scalogram of these two variables represents the response of q_c to the CTKE excitation or the *energy flux* from the coherent velocity field to the blade as manifested by the time variation of q_c. The fluctuating dynamic pressure excites the blade modal frequencies many of which are lightly damped. This results in the storing and propagation of vibrational energy within the remainder of the turbine structure.

We demonstrate this process in Figure 2 where we plot the interaction between the local CTKE and q_c at the 78% blade span station for the modeled WindPACT rotor. The upper panel displays the time series of the CTKE in red and the q_c in blue. The time-frequency variations of the energy content of each of these variables are shown in the two panels immediately below and variation of the energy transport or flux between CTKE and q_c is displayed in the lowermost panel. In this short record, the 78% blade span station encounters an intense region of CTKE with a peak value of almost 40 m^2/s^2 between 25 and 30 seconds into the record. While the most intense flux of energy (dark red in lowermost panel) from the coherent turbulence to the blade is found in the lowest frequencies, transfers also occur at the higher frequency vibrational modes in Table 1 (greater than ~ 3 Hz). These are somewhat difficult to see because of the non-linear frequency scale. This process can be described as a *resonant coupling* between the spatiotemporal structures in the coherent turbulent inflow field and vibrations created within the blade structure as a result of the lightly damped structural modes. We believe this explains the 1:1 correspondence we observe in the spectral frequencies of the coherent turbulence field and the vibratory response of the turbine blades discussed in [3] and illustrated in Figure 2.

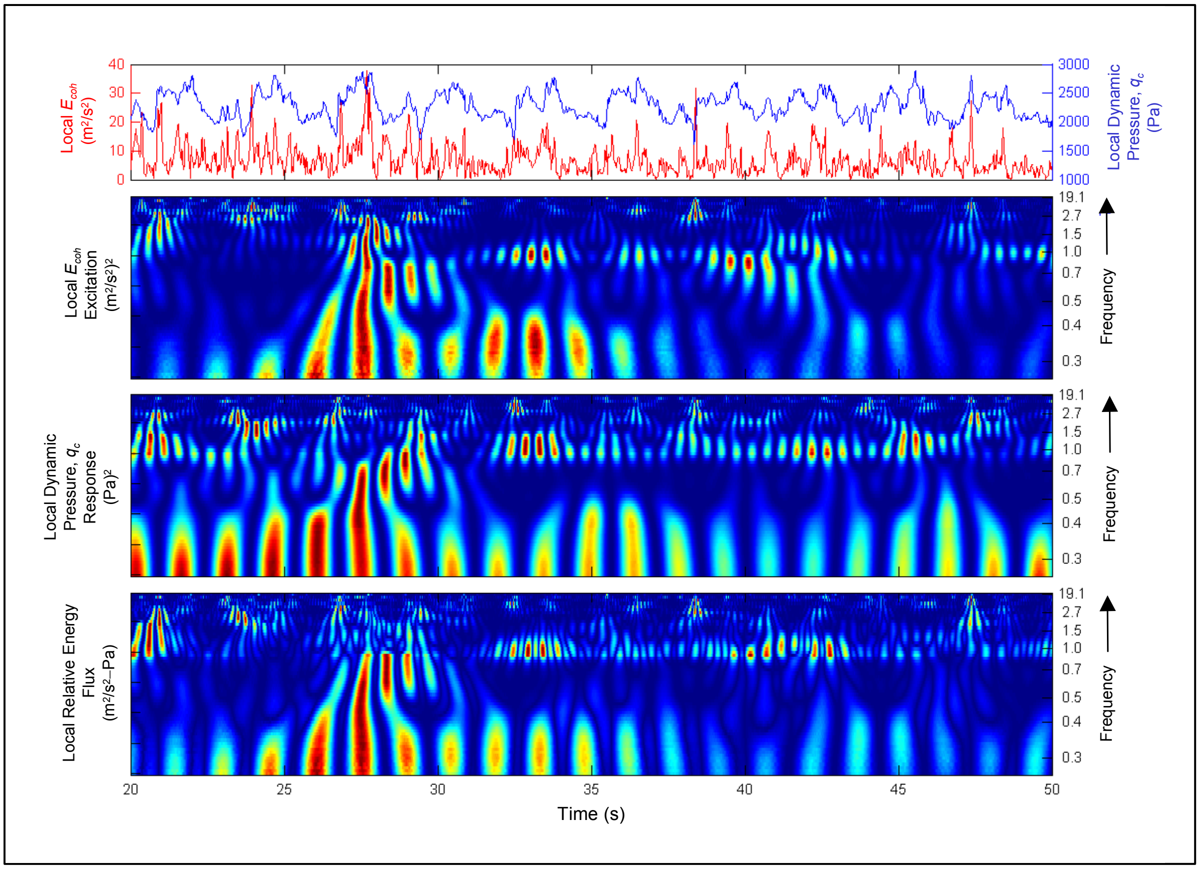

Figure 2. Spectral flux of coherent turbulent energy from a breaking KH billow to the WindPACT rotor blade at the 78% blade span station.

The spatiotemporal characteristics of the turbine inflow turbulence field are very important in determining not only the aeroelastic response of the blades but the rate and intensity in which turbulent energy is transferred from the turbulence to the rotor and subsequent structure. To demonstrate this we again use the virtual WindPACT turbine model by exciting it with simulated inflow turbulence fields generated: (**1**) in accordance with the specifications of the IEC Kaimal Normal Turbulence Model (NTM) and the Normal Wind Profile (vertical shear exponent of 0.2) [9]; (**2**) stable flow above flat, homogenous terrain with an intense vertical shear exponent of 1.49 but no small-scale coherent turbulent structures; and (**3**) the breakdown of the KH billow with an initial shear exponent of 1.49 (the shear decreases during the breakdown because of the intense vertical mixing that takes place).

In Figure 3, we compare the energy flux from coherent turbulence to the blade dynamic pressure at the 78% span station of the WindPACT turbine model for the three inflows defined above. We present the information similarly to the lowermost panel of Figure 2 but in a 3-dimensional format with the magnitude of the energy flux logarithmically scaled by height on the vertical axis and not as shades of red and blue. An examination of the three graphs reveals that there is at least an order of magnitude greater energy flux up to the highest frequencies with the breaking KH billow in the inflow (Figure 3-c) as compared with the IEC NTM (Figure 3-a) and highly-shear stable flow (Figure 3-b). The IEC NTM inflow transports a smaller but significant energy flow into the turbine rotor up to about 3-4 Hz but then decreases rapidly at higher frequencies in comparison with the KH billow breakdown and its intense, small-scale coherent structures. The stable, highly sheared flow (Figure 3-b) creates similar levels of flux as the KH billow at the lowest frequencies because of the strong wind shear. The flux then decreases rapidly with increasing frequency as a consequence of the lack of coherent turbulent structures. These three diagrams illustrate, at least in terms of the flux of energy from the turbulent inflow to the turbine rotor blades, that the character and structure of the inflow is very important in determining turbine structural response.

Figures 2 and 3 show that turbine rotor blades passing through patches of coherent turbulence will experience the transient excitation of higher frequency vibrational frequencies that, according to Table 1, may interact with the dynamics of the turbine tower and probably with other components that are not being accounted for in the model of this virtual turbine. It is unlikely that the entire kinetic energy coupled into the rotor blades will be converted into electrical power particularly at the higher frequencies. It is more likely that this high frequency energy will be dissipated as it propagates through the structure with the exact path and degree of local dissipation being a function of the specific turbine design and construction details. We schematically diagram the spectral energy distributions associated with this process in Figure 4. The spectrum of total turbulent energy is outlined as the upper curve boundary where peak energy occurs on the order of one minute or less. The hatched area indicates the spectrum of the turbulent energy that is converted to electrical energy. The remaining solid area represents the *parasitic* energy that must be dissipated by the structure and components. Thus the turbine and its components must be designed to adequately accommodate the

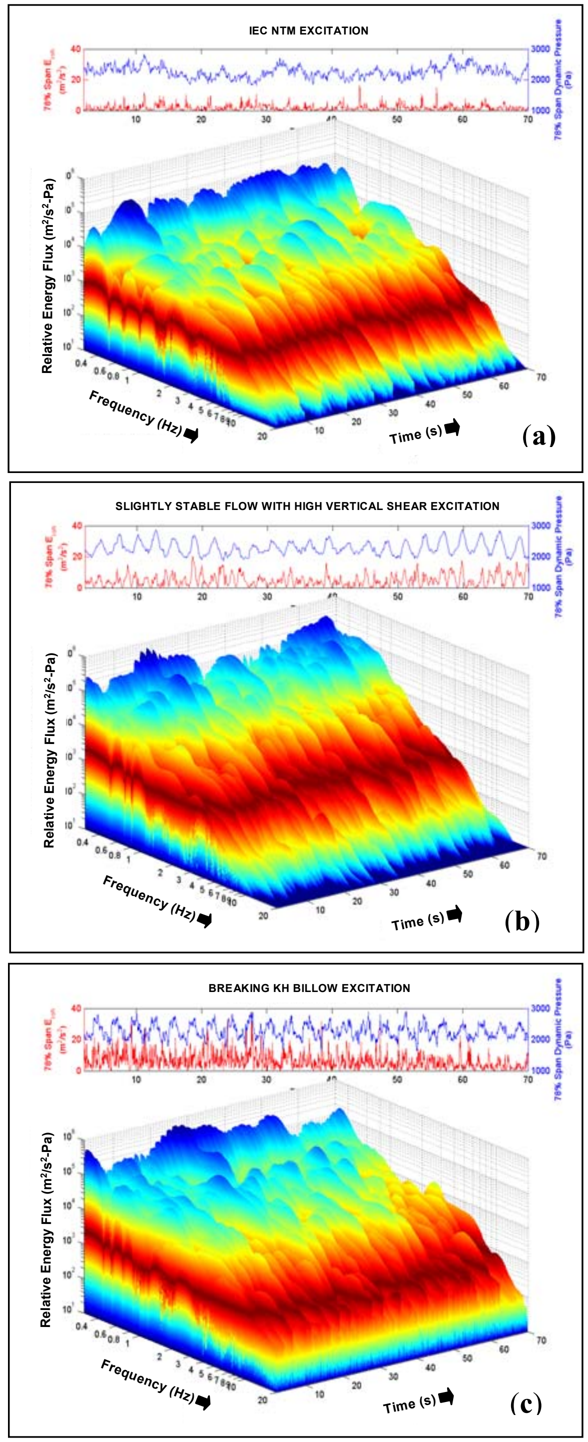

Figure 3. Spectral flux of coherent turbulent energy (CTKE or E_{coh}) to blade dynamic pressure (q_c) at 78% span for inflows of: (**a**) IEC NTM, (**b**) stable flow with high shear, and (**c**) breaking KH billow.

dissipation of induced parasitic energy over its design lifetime. As is sketched in Figure 3-c, the greater the percentage of time the turbine operates in coherent turbulence the larger the un-hatched area of Figure 4 and the greater the need to accommodate that in the turbine design.

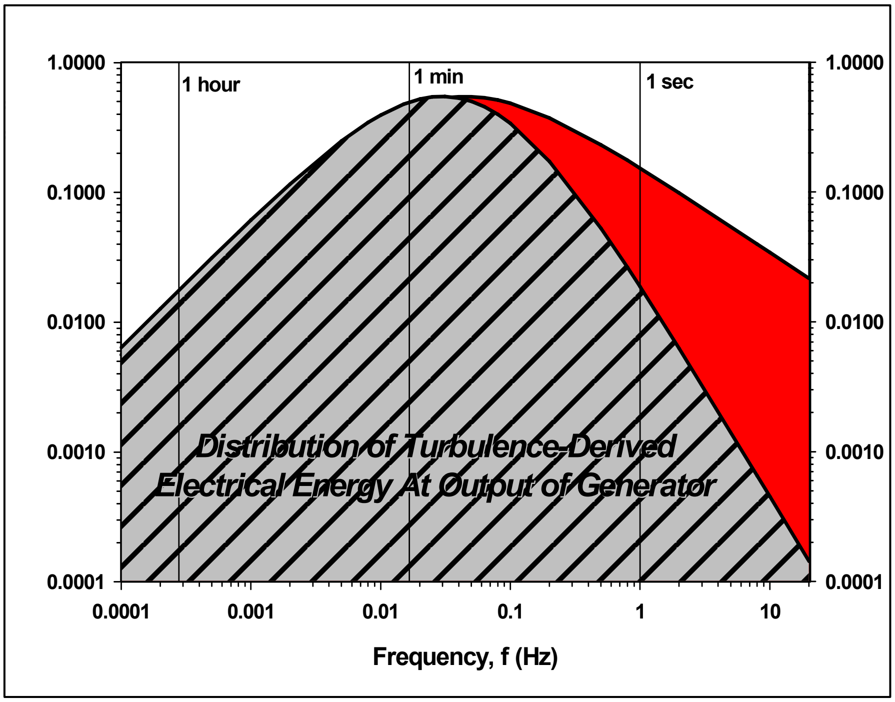

Figure 4. Schematic of spectral relationship between turbulent energy appearing at output of generator as electrical energy and the total available turbulent energy.

Propagation of Coherent Turbulent Energy

As part of the Long-Term Inflow and Structural Testing (LIST) Program conducted by NREL and Sandia Laboratories, we made detailed measurements of the both the inflow and response of the NWTC Advanced Research Turbine (ART) [10]. The ART turbine is an upwind, two-bladed 600-kW machine. It has a teetered hub at a height of 37 m and a full-span pitch controlled, 43-m diameter rotor that operates at 42 rpm. We measured the detailed characteristics of the turbulent inflow using an upwind planar array of five high-resolution sonic anemometers with spatial dimensions equivalent to the turbine rotor disk. The turbine measurements included an inertial measurement unit (IMU) that was mounted on the forward low-speed shaft support bearing and immediately downwind of the rotor. It consists of an orthogonal triad of inertial-grade accelerometers and rate gyroscopes whose axes of rotation were aligned with the measurement directions of the accelerometers; i.e., fore-aft (X), side-to-side (Y), and vertical (Z). The means of the accelerations were removed, and the remainder was integrated twice to provide time histories of acceleration, velocity, and displacement for each of the measurement axes over a 10-minute record.

We have previously discussed, using the numerical simulations, the process of the flow of turbulent kinetic energy into the rotor blades caused by resonant coupling with the coherent turbulence and the vibrational frequencies of the blades. With actual measurements collected from the ART turbine, we can now examine the transport or flux of vibrational energy from the blade roots into the low-speed shaft and in the zero-mean bending loads of the shaft itself. We also have detailed measurements of the vibrational frequencies or modes that were acquired from a sister machine (the Controls Advanced Research Turbine [CART]) by Osgood, et al [11,12] whose primary structural details are essentially identical. These are listed in Table 2. In addition to the modal frequencies and their nominal source characteristics, measured values of

TABLE 2. CART (ART) Turbine Measured & Calculated Static System Frequencies

Frequency Range (Hz)	Vibrational Modes General Characteristics	Range of Measured % Critical Damping	Total Number of Included Modes[§]	Number of Blade/Tower/ Drivetrain Interacting Modes[#]
0.716	1-P	–	–	–
0.867 – 0.886	Blade 1st bending, tower 1st fore-aft bending, drivetrain bending	0.68 - 2.66	7	3
1.390 – 1.580	Blade 1st bending, tower side-side bending, drivetrain lateral bending	0.74 – 1.52	3	2
2.060 – 2.081	Blade 1st & 2nd bending	0.70 – 0.93	3	0
3.886 – 4.451	Blade 1st & 2nd bending, drivetrain lateral bending, tower torsion	0.70 – 0.72	6	7
5.050 – 6.810	Blade bending, drivetrain, tower lateral & torsion	0.24 – 0.95	8	10
7.815[#] – 8.411[#]	Blade bending, tower fore-aft & lateral bending, drivetrain bending	*n.a.*	2	3
9.0[§] – 10.84[§]	Blade bending, drivetrain interaction	*n.a.*	2	1

[§]*measured plus modes from FAST model eigenanalysis*
[#]*modal interactions estimated from FAST model eigenanalysis only*

the corresponding damping ratios and the indication of modal interactions with the blades, tower, and drivetrain are provided as opposed to only the blades and tower in the WindPACT Model. The original analysis of the CART modal survey [11] only resolved modal frequencies up to about 6 Hz. Our analysis of the long-term inflow and structural testing (LIST) measurements revealed the apparent presence of modes approaching 11 Hz. As a result, Osgood [12] performed additional analyses of the original modal survey data in which he paid particular attention to tests in which the entire turbine structure was excited by employing both a “snap-back” of the tower and nacelle and by the turbulent wind itself. He confirmed the existence of these higher frequency vibration modes but was not able to obtain reliable estimates of their modal damping.

We used the FAST Model of the ART developed by A. Wright of NREL to calculate vibrational frequencies seen in the LIST measurements and modal survey. These served as a validation of the model’s ability to reproduce the entire measured range of modal frequencies in its solutions and to establish the characteristics of the highest frequency modes and their interactions. Clearly there are more modal frequencies and modal interactions in Table 2 as compared with the virtual turbine in Table 1. These results underscore the benefit of performing a detailed modal survey on turbine prototypes as part of the development process. Note also the increase in the number

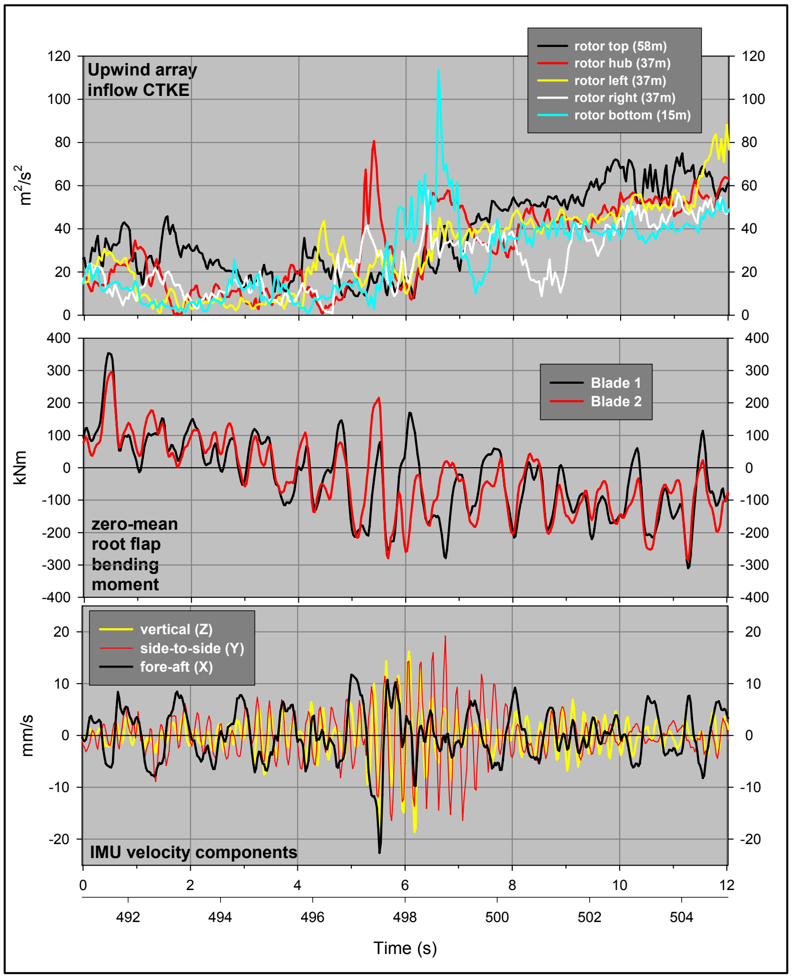

Figure 5. Array inflow and turbine response time histories associated with an observed intense coherent event on the ART turbine.

of modes (*modal density*) and modal interactions with increasing frequency within the bandwidth of the measurements. This trend undoubtedly continues into the calculated range of higher frequencies, but they could not be adequately resolved with the linear eigenanalysis technique employed.

We can now demonstrate the process of vibration energy propagation described above using actual measurements from the LIST Experiment and the NWTC ART Turbine. In Figure 5, we examine the details of the interaction of the turbine rotor and its drivetrain with an intense coherent turbulent inflow structure as described by the upwind array of five sonic anemometers [10]. This inflow event occurred in a slightly stable inflow at 5 a.m. mountain standard time (MST) on May 5, 2000. The time histories of the CTKE, as measured by each of the five sonic anemometers, are plotted in the topmost panel of Figure 5. This event occurred between about 496 and 500 seconds into a 600-second record. A second time axis, with zero at the beginning of the segment, is provided as a more sensitive relative time scale. The time histories of the zero-mean root out-of-plane (OP) bending moments are displayed in the center panel while the time variations of the zero-mean fore-aft (X), side-to-side (Y), and vertical velocities (Z) measured by the IMU atop the forward low-speed support bearing are provided in the lowermost panel.

The actual inflow event lasts about 2 seconds and, as can be seen from the plot, is quite complex. The two large CTKE peaks suggest that the spatial dimensions of the actual coherent structures are much smaller than the rotor disk and something our simulations of breaking KH billows has demonstrated. An examination of the histories in the center panel reveals that the large load excursion in Blade 2 occurs at about 5.5 seconds into the plotted record and appears to be related to the 80 m^2/s^2 CTKE peak measured upstream at the equivalent rotor hub center position. A similar peak then occurs in the load history of Blade 1, suggesting that the coherent structure was extended in time and space sufficiently for both blades to pass through it. Other analyses described in [10] suggest that the structure was propagating towards the ground as well as moving horizontally and probably is the source of the even larger CTKE peak measured about a second later at the height of the lowest-level anemometer (15 m). At that point, its severity appears not to have had much impact on the turbine rotor as it is likely it was below the lowest elevation of the rotor plane by the time it reached it or simply did not intersect one of the blades. The large excursion in the fore-aft (X) local velocity component of the forward support bearing shown in the bottom panel is also highly correlated in time with the hub-center CTKE event by first moving downwind (+10 mm/s) and then rapidly upwind (-21 mm/s) over a period of about one second. At nearly the same time, a higher-amplitude oscillatory behavior in the side-to-side (Y) and vertical (Z) velocity components also is initiated with the oscillations in the Y-velocity component lasting the longest. The dominant frequency of these oscillations is in the neighborhood of 6 Hz and is arrived at by visually counting the peaks shown in Figure 5 for a period of one second. The dynamic activity at this frequency compares favorably with the number of low-damped vibration modes and the high number of complex modal interactions between the blades, the tower, and the drivetrain listed in Table 2.

In Figure 6, we illustrate the observed time-frequency variation of the propagation or flux of vibrational energy between the ART root bending loads and the low-speed shaft during the rotor's encounter with the intense coherent turbulent structure depicted in the time histories of Figure 5. This presentation, using the wavelet co-scalogram, allows us to examine the time variation of the intensity *and* frequency content of the flow of vibrational kinetic energy as the blade passes through a coherent turbulent structure. From Figure 5, we noted that the impact of this encounter was applied over a period of about 2 seconds but we could not ascertain what the spectral content of the energy flow between the blade roots and the low-speed shaft was and therefore what modal frequencies may be involved. In Figure 6, we present this interaction between the blade root in-plane (IP) (Figure 6-a) and OP bending loads (Figure 6-b) and the low-speed shaft expressed in terms of the zero-mean X, Y, and Z velocities measured on the forward support bearing and the zero-mean bending loads on the shaft itself. The impulsive nature of this encounter is well demonstrated in this presentation. The lowest row of diagrams in each figure display the intensities and frequencies in which the vibrational energy is flowing during the event. With the exception of the side-to-side (Y) velocity, energy is flowing across a wide or *broadband* frequency range that is consistent with the application of a short-period, impulsive load. By comparison, the side-to-side (Y) energy flow is dominated in a *narrowband* range of frequencies in the vicinity of 6 Hz. As previously pointed out, this frequency range includes a high number of interacting vibrational modes some of which are very lightly damped (Table 2) and therefore capable of storing greater amounts of energy. While this experiment did not include the measurement of bending loads on the tower, we would expect similar depictions to those shown in Figure 6.

Effect of Increasing Blade Structural Damping

The small structural damping associated with many of the blade modal frequencies (mode shapes) shown in Table 2 allows more vibrational energy to be stored particularly under the short-period or impulsive loading as a result of encountering intense, coherent turbulent structures in the inflow as demonstrated above. The energy flux from encountering coherent

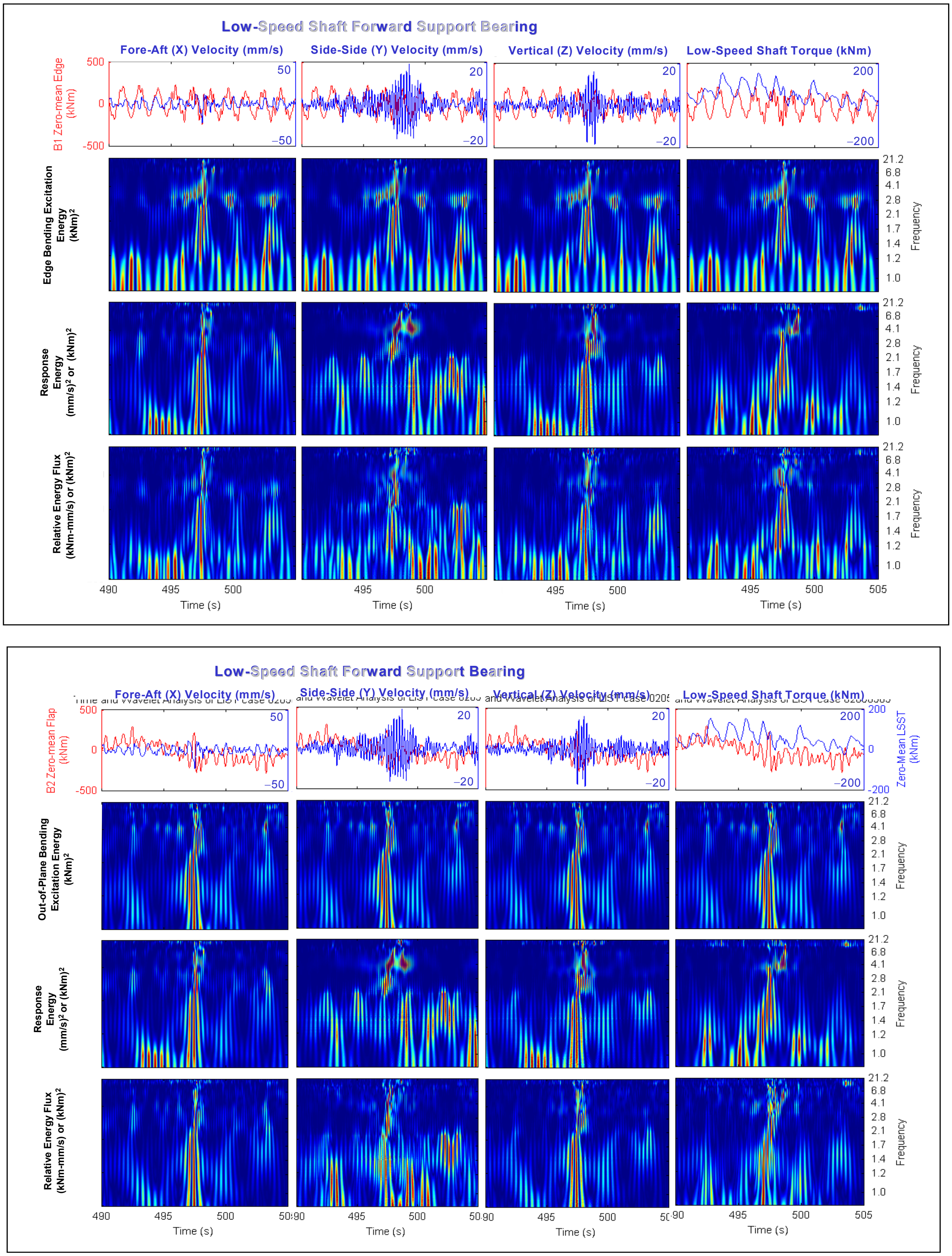

Figure 6. Observed vibrational energy propagation between (**a**) in-plane and (**b**) out-of-plane blade root loads and IMU X-, Y-, and Z-velocities and low-speed shaft bending loads.

turbulent events creates an additional reservoir of energy that, if not converted into usable electrical power, must be dissipated somewhere in the structure or ultimately in the foundation should it reach it. The 600-kW ART is relatively small by today's standards, but several of the higher order blade modes are lightly damped (less than 0.5% of critical according to Table 2). We expect a further decrease in damping for blades constructed for turbines the size of the 1.5-MW WindPACT turbine and larger. In the FAST model of the virtual WindPACT Turbine we used values suggested by A. Wright of 0.3% of critical for the first two OP bending modes and 0.5% for the first IP mode. These seem reasonable compared with the measured values of 0.6% to 0.7% for the ART blade, which is about 40% smaller in length and less than 60% of the mass of the WindPACT virtual blade.

To access the influence of the degree of structural blade damping, we recalculated the WindPACT turbine original simulation whose results are plotted in Figure 2. This time we increased the blade structural damping used by about an order of magnitude or 3.88% for the OP modes and 5.9% for the IP. We compared the predictions for the three excitations used to generate Figure 3 (the IEC Kaimal NTM, the stable, highly sheared flow, and the breaking KH billow) the results of which are summarized in Figure 7. In this figure, we plot the energy flux from the CTKE to the dynamic pressure, q_c, at the blade 78% span station similar to Figure 2 for each of the three excitations (as rows) and the two levels (as columns) of blade structural damping. The colors representing the intensity of the flux have been scaled relative to the observed range for all three excitations for a given damping level and with deep red again representing the highest level of energy transfer. This presentation method provides a better visual comparison of the relative intensities of fluxes created with each of the three excitations. Clearly the IEC NTM is the least severe of the three while the breaking KH billow creates the greatest energy flux into the blade at both damping levels. There is no discernable difference in the level of energy flux for both the IEC NTM and stable, sheared flow excitations. However, there is a noticeable reduction in the severity of the flux with the higher damping when excited by the breaking KH billow. This is particularly true with the intense coherent event seen between 25 and 30 seconds as evidenced by the smaller areas of intensive flux (energy being transferred at fewer modal frequencies) for the blade with increased structural damping. Thus it may be possible to reduce the flux of parasitic vibrational energy into the turbine structure under coherent turbulent loading by increasing the structural damping in the design of large blades.

SIMULATING COHERENT INFLOW TURBULENCE

Clearly from the previous discussion, it is very important that the simulated inflow turbulence fields needed to excite numerical simulations of turbine dynamics contain spatiotemporal coherent features. Without these features, the amount of higher frequency vibrational energy created by the simulated inflow may be as much as an order of magnitude less than occurs when coherent turbulent structures are present. Further, coherent structures induce short-period or impulsive loading events whose consequences may be detrimental to various subsystem components during both short and long periods of time, depending on the characteristics involved. Thus, turbine simulations intended to isolate potential high-stress areas or to obtain estimates of component or entire system lifetimes need to include inflow simulations with these coherent features with a frequency of occurrence derived from observations for a specific site or class of sites.

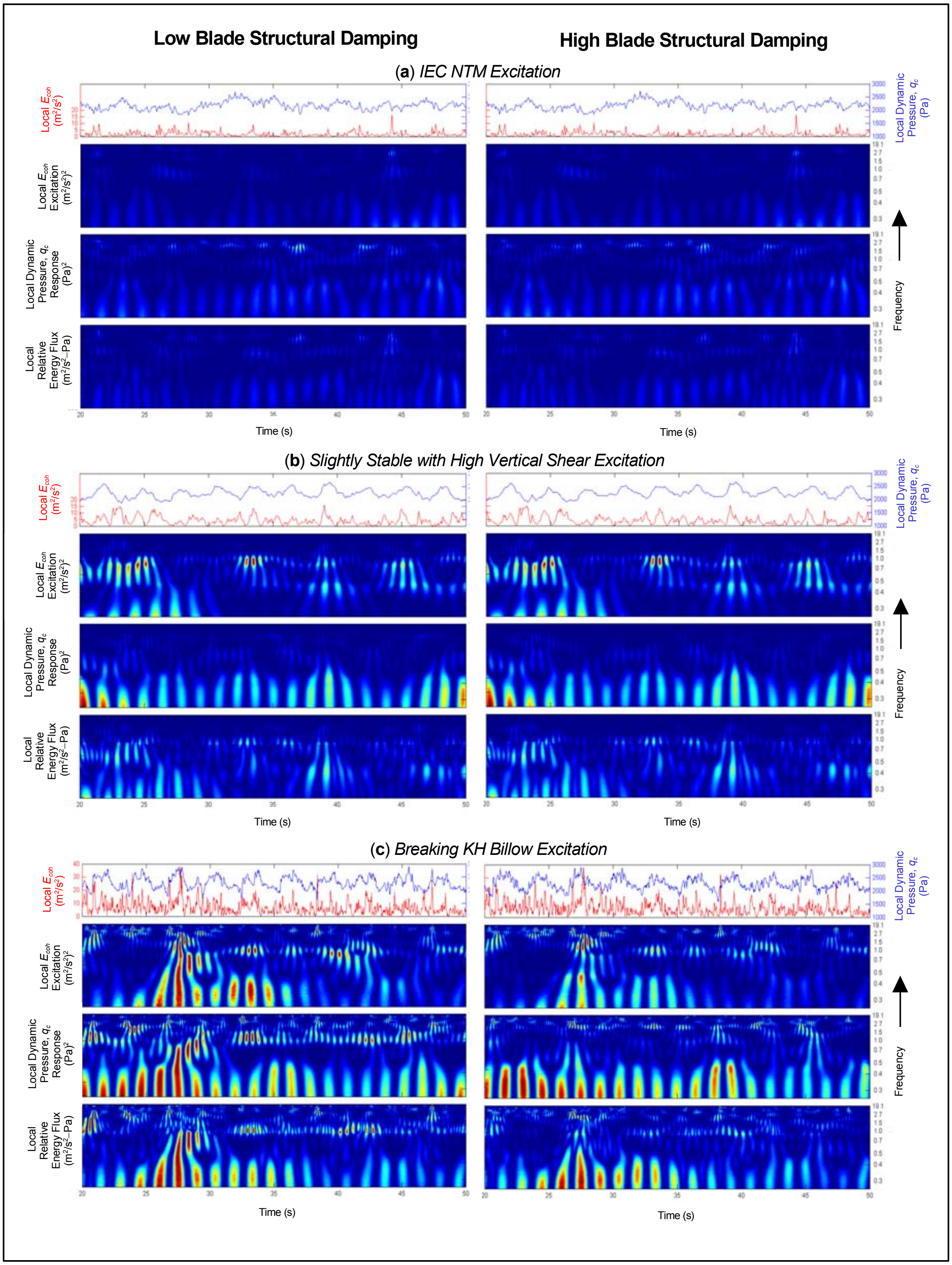

Figure 7. Comparison of the level of flux of coherent turbulent energy from inflow excitations from: (**a**) IEC Kaimal NTM, (**b**) stable, highly sheared flow, and (**c**) a breaking KH billow to the WindPACT rotor blade at the 78% blade span station for low and high structural damping.

We are in the process of developing a turbulent inflow simulator code that will reflect a wide range of turbine inflow conditions including at least two general site-specific environments with validated simulation of flows containing spatiotemporal coherent turbulent structures. Our *TurbSim* inflow simulator code can statistically simulate a wide range of inflows including that specified by the IEC Kaimal NTM and the inflow characteristics observed at the NWTC. In the near future, it will also simulate conditions associated with the operation of large wind turbines in the presence of a nocturnal low-level jet stream.

We developed the *TurbSim* stochastic inflow turbulence code to provide a numerical simulation of a full-field flow that contains coherent turbulence structures that reflect the proper spatiotemporal turbulent velocity field relationships seen in instabilities associated with nocturnal boundary layer flows and that not represented well by the IEC Normal Turbulence Models (NTM). Its purpose is to provide wind turbine designers with the ability to drive design code (FAST or MSC.ADAMS®) simulations of advanced turbine designs with simulated inflow turbulence environments that incorporate many of the important fluid dynamic features known to adversely affect turbine aeroelastic response and loading.

The *TurbSim* code is based on the original stochastic wind simulator code *SNLWIND* [13], developed by Paul Veers at Sandia National Laboratories, that uses the *spectral representation* method to generate wind fields in the time domain and is often referred to as the "Veers Method". Veers' original code only simulated the streamwise component of the wind within a polar or Cartesian grid as a function of time in a neutral atmosphere. Kelley [14] expanded the code to generate a flow that includes three wind components (streamwise, crosswind, and vertical) in a diabatic (non-neutral) atmosphere under various site-specific conditions including over smooth, homogenous terrain and upwind, within, and downwind of a multi-row wind farm. Later Buhl [15] took Kelley's version and optimized it to simulate winds prescribed by the International Electric Commission (IEC) neutral flow specifications. The latest release of *TurbSim*, which provides IEC-specified inflows and those mentioned previously, also includes the ability to generate a turbulent inflow that is *statistically characteristic* of the highly turbulent conditions experienced when testing turbines at the NWTC; i.e., downwind of a major mountain range. It represents a test environment corresponding to those found in complex terrain situations that often present challenges for turbine operations.

The *TurbSim* code *efficiently* generates *randomized* coherent turbulent structures that are superimposed on a stationary background turbulent field. The background turbulence is generated by Veers' spectral representation method using Fourier inversion of one of the furnished turbulence spectral models. The non-stationary, coherent turbulent structures are, in effect, then added to this flow field in the time domain. These structures exhibit the correct temporal and spatial phase relationships associated with the flow elements of the breakdown of a stationary Kelvin-Helmholtz (KH) wave or billow. The structures, whose intensity, length, and position are random variables, are scaled by the specified boundary conditions. They are composed of a series of individual coherent events that have been isolated from the NCAR LES or a direct numerical simulation (DNS) of a KH Billow. The DNS simulation by Werne and Fritts [16] was used as the prototype by NCAR for their effort but, unlike NCAR's stationary billow solution, their billows propagate with time. It includes smaller- scale motions but generally produced similar results. We noticed a few subtle differences in the flow structures generated by the DNS version compared with the LES that we decided to incorporate in *TurbSim*. Fourteen non-dimensionalized, spatiotemporal coherent flow structures were isolated from the breakdown of the LES KH billow and six from the DNS. Figure 8 illustrates the superposition of the streamwise, crosswind, vertical wind components of a coherent turbulent structure (red) onto a more random turbulent background that form the 50 m^2/s^2 CTKE or E_{coh} peak about 350 seconds into the record. What is not shown is the spatiotemporal relationship that exists between the wind components of the superimposed turbulent structure seen at this location and the remainder of its organized spatial extent that the turbine blades may or may not encounter as they rotate.

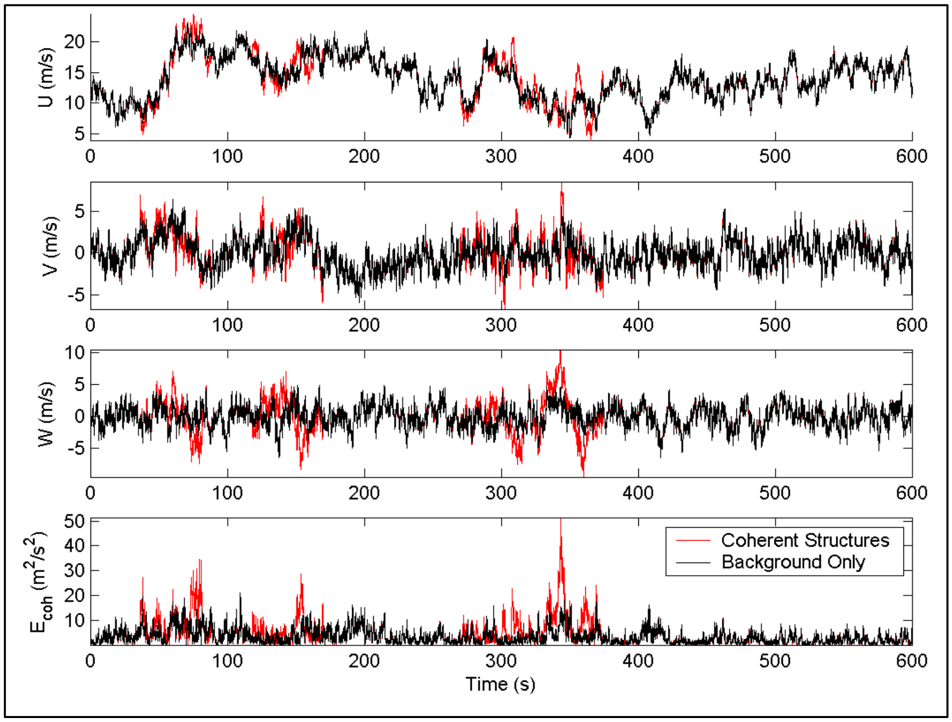

Figure 8. Example of coherent turbulent structure of intensity CTKE (E_{coh}) being added to the streamwise (U), crosswind (V), and vertical (W) wind components at a given grid point location.

Turbulence is a stochastic process. The IEC NTM assumes that the statistics of the turbulence are stationary and the velocities are at least, to a first approximation, normally or Gaussian distributed. This is consistent with the application of the Kaimal turbulence spectral model in which the turbulence process is assumed in equilibrium; i.e., turbulent production is in balance with dissipation. The presence of a breaking KH billow represents a non-stationary process in which short period statistics (including spectral energy) vary with time and position (non-homogeneous) and turbulence production and dissipation are not in balance. This is why we must simulate the coherent turbulence process in the time domain by adding or superimposing it onto the turbulent background that is varying very slowly with respect to the length of the simulated record (typically 10 minutes) . We examined the statistics of the coherent event process by analyzing the statistics of such events derived from the LIST upwind array measurements. Many of the stochastic attributes of these events can be nominally described by parametric exponential, Poisson, or lognormal probabilistic processes. For example the time within a 10-minute record where a coherent structure occurs can be modeled by a Poisson process in which the rate of occurrence is not constant; i.e., *non-homogeneous*. We found that

TABLE 3. Comparison of Maximum Number of Probabilistic Degrees of Freedom for *TurbSim* Spectral Models for a Given Set of Specified Inflow Boundary Conditions

Spectral Model	Max Probabilistic Degrees of Freedom	Number of Spectral Peaks per Stability Class
IEC Kaimal	1	1 (neutral)
"Smooth" Terrain	7	2 – unstable, 1 –neutral, stable
Wind Farm	7	3 – unstable, 2 –neutral, stable
NWTC (complex terrain)	9	2 – unstable, 2 – neutral, stable
GP_LLJ	?	?

this observed rate could be scaled in terms of vertical stability and the mean hub-height wind speed. The expected length of coherent events was found to be lognormally distributed and scaled with the height above the ground. To achieve the highest level of statistical agreement between the inflow measured by the LIST array and our simulations, it was necessary to incorporate nine probabilistic degrees of freedom. Table 3 summarizes the number of statistical degrees of freedom available for each of the turbulence spectral models provided by *TurbSim*. The number of spectral peaks for a given model refers to the distinct peaks incorporated within that model and under what stability conditions. The GP_LLJ is a future model that refers to spectral models characteristic of sites within the Great Plains and associated with the presence of a low-level jet stream. We will be using the year of turbulence measurements collected by the Lamar Low-Level Jet Project [2] to develop the models.

TurbSim is intended as an integral part of a Monte Carlo simulation of wind turbine dynamics. It is used to generate a series of inflow realizations for a given set of initial boundary conditions that are applied as input flow fields to turbine design codes (FAST or MSC.ADAMS®) to produce response (load) solutions that can be analyzed using ensemble statistics. A minimum of 31 realizations is recommended for a specific set of boundary conditions to allow the use of large sample statistics and to obtain expected distributions of turbine response parameters under various types of inflow loading.

CONCLUSIONS

We have shown using both numerical simulations and actual measurements that a resonant coupling of energy occurs between coherent turbulent fields and the natural vibrational modes of a turbine rotor blade as it passes through coherent turbulent structures. These organized structures frequently develop in the nocturnal boundary layer as a result of Kelvin-Helmholtz Instability (KHI) associated with the presence of low-level jet streams. This resonance induces a flow or flux of turbulent kinetic energy into the blade structure that is propagated into the remainder of the turbine. The spatiotemporal characteristics of a coherent turbulent field are very important in determining the amount of energy that does not appear at the generator terminals and must be dissipated by the turbine structure. We demonstrated that simulations that use the IEC NTM are deficient in the flux of high frequency turbulent energy into the blade and turbine structure and therefore underestimate the amount of vibrational energy that must be dissipated before they reach the turbine structural components. The total dissipative energy that is not being accounted for will depend on the number of simulations run and how many of those contain coherent turbulence structures as compared with only using the IEC NTM excitation. We also saw that increasing the effective structural damping in turbine blades may be an avenue to reducing turbulent energy flux into the turbine and require less energy to be dissipated.

The *TurbSim* Code provides the turbine designer with the ability to assess the flow of vibrational energy through the modeled turbine components under coherent turbulent loading. It also provides a means to estimate how much energy will need to be dissipated and to choose what methods to use to accommodate it to increase component lifetimes and reliability.

ACKNOWLEDGEMENTS

This work is supported by the U.S. Department of Energy under contract No. DE-AC36-83CH10093. We want to thank the Office of Wind and Hydropower Technologies for supporting this effort.

We also want to thank our NREL colleagues Jason Jonkman, Dr. Alan Wright, Richard Osgood, and Marshall Buhl for their support and cooperation in this work.

REFERENCES

1. Kelley, N.D. (March 2004). "An Initial Overview of Turbulence Conditions Seen At Higher Elevations Over the Western Great Plains," *Global Windpower 2004 Conference Proceedings* (CD-ROM), 28-31 March 2004, Chicago, Illinois. Washington, DC: American Wind Energy Association; Omni Press; 12 pp.; NREL Report No. CP-500-35970.

2. Kelley, N.; Shirazi, M.; Jager, D.; Wilde, S.; Adams, J.; Buhl, M.; Sullivan, P.; Patton, E. (2004). *Lamar Low-Level Jet Program – Interim Report*. National Renewable Energy Laboratory. Golden, CO. NREL/TP-500-34593. 216 pp.

3. Kelley, N.D.; Osgood, R.M.; Bialasiewicz, J.T.; Jakubowski, A. (July-September 2002). "Using Wavelet Analysis to Assess Turbulence /Rotor Interactions." *Wind Energy* (3:3), pp. 121-134.

4. Malcolm, D.J.; Hansen, A.C. (August 2002). *WindPACT Turbine Rotor Design Study*. Global Energy Concepts LLC and Windward Engineering for the National Renewable Energy Laboratory. Golden, CO. NREL/TP-500-34593, 71 pp.

5. MSC.Software Corporation. *ADAMS/Solver Task Documentation Kit. Version 12.0* MSC.Software Corporation, Santa Ana, CA.

6. Jonkman, J. M.; Buhl, M.L. (March 2004). *FAST Users Guide*. National Renewable Energy Laboratory. Golden, CO. NREL/EL-500-29798, 95 pp.

7. Jonkman, J.; Cotrell, J. (2003). *Demonstration of the Ability of RCAS to Model Wind Turbines*. National Renewable Energy Laboratory. Golden, CO. NREL/TP-500-34632. 59 pp.

8. Gurley, K. and Kareem, A. (1999). "Applications of Wavelet Transforms in Wind, Earthquake, and Ocean Engineering." *Engineering Structures* (21:2), pp. 149-167.

9. International Electrotechnical Commission. (1998) *Safety of Wind Turbine Conversion Systems.* 61400-1, 2ed. http://www.iec.ch.

10. Kelley, N.; Hand, M; Larwood, S.; McKenna, E. (January 2002). "The NREL Large-Scale Turbine Inflow and Response Experiment – Preliminary Results." Prepared for the 21st ASME Wind Energy Symposium. Reno, NV. January 14-17, 2002. NREL/CP-500-39017. Golden, CO: National Renewable Energy Laboratory, 15 pp.

11. Osgood, R.M.; McFarland, H.G.; Johnson, G.L. (February 2002). *Full System Modal Survey Test Results of the Controls Advanced Research Turbine (CART) Located at NWTC Site 4.3*. National Renewable Energy Laboratory. Golden, CO. NREL Internal Letter Report. 39 pp.

12. Osgood, R.M. (June 3, 2004). *CART Natural Frequency Snap-back Test Report, April 24-26, 2001*. National Renewable Energy Laboratory. Golden, CO. NREL Internal Draft Report. 14pp.

13. Veers, P.S. (March 1988). *Three-Dimensional Wind Simulation*. Sandia National Laboratories. Albuquerque, NM. SAND88-0152. 36pp.

14. Kelley, N.D. (November 1992). *Full Vector (3-D) Inflow Simulation in Natural and Wind Farm Environments Using An Expanded Versions of the SNLWIND (Veers) Turbine Code*. National Renewable Energy Laboratory. Golden, CO. NREL/TP-442-525. 8 pp.

15. Buhl, M. L., Jr. (2001). "SNwind User's Guide (v1.0)". NREL Report No. EL-500-30121. 4 pp.

16. Werne, J.A.; Fritts, D.C. (1999). "Stratified Shear Turbulence: Evolution and Statistics." *Geophys. Res. Lett.* (26), pp 439-442.

REPORT DOCUMENTATION PAGE

Form Approved
OMB No. 0704-0188

1. REPORT DATE *(DD-MM-YYYY)*
August 2005

2. REPORT TYPE
Conference Paper

3. DATES COVERED *(From - To)*

4. TITLE AND SUBTITLE
The Impact of Coherent Turbulence on Wind Turbine Aeroelastic Response and Its Simulation: Preprint

5a. CONTRACT NUMBER
DE-AC36-99-GO10337

5b. GRANT NUMBER

5c. PROGRAM ELEMENT NUMBER

6. AUTHOR(S)
N.D. Kelley; B.J. Jonkman, and G.N. Scott

5d. PROJECT NUMBER
NREL/CP-500-38074

5e. TASK NUMBER
WER5.3105

5f. WORK UNIT NUMBER

7. PERFORMING ORGANIZATION NAME(S) AND ADDRESS(ES)
National Renewable Energy Laboratory
1617 Cole Blvd.
Golden, CO 80401-3393

8. PERFORMING ORGANIZATION REPORT NUMBER
NREL/CP-500-38074

9. SPONSORING/MONITORING AGENCY NAME(S) AND ADDRESS(ES)

10. SPONSOR/MONITOR'S ACRONYM(S)
NREL

11. SPONSORING/MONITORING AGENCY REPORT NUMBER

12. DISTRIBUTION AVAILABILITY STATEMENT
National Technical Information Service
U.S. Department of Commerce
5285 Port Royal Road
Springfield, VA 22161

13. SUPPLEMENTARY NOTES

14. ABSTRACT *(Maximum 200 Words)*
In this paper, we present a brief overview of our recent research results regarding the impact of organized or coherent inflow turbulence on the dynamic response of operating wind turbines. Previous field experimentation has demonstrated that the greatest structural fatigue damage tends to occur during the nighttime hours from coherent turbulence that develops in the stable, nocturnal atmospheric boundary layer. We have found that under such conditions, intense vertical wind shear and temperature gradients create resonant flow fields that are capable of imparting short-period loading and vibrational energy as wind turbine rotor blades pass through regions of organized or coherent turbulence. This energy is subsequently propagated throughout the remainder of the structure, where it is often locally dissipated. We also briefly discuss our recent progress in developing a numerical simulation that includes such coherent inflow conditions that can be used to excite wind turbine design codes.

15. SUBJECT TERMS
wind power; wind plants; utility system; electric power system

16. SECURITY CLASSIFICATION OF:			17. LIMITATION OF ABSTRACT	18. NUMBER OF PAGES	19a. NAME OF RESPONSIBLE PERSON
a. REPORT	b. ABSTRACT	c. THIS PAGE			
Unclassified	Unclassified	Unclassified	UL		19b. TELEPHONE NUMBER (*Include area code*)